doi:10.1016/S0022-2836(02)01068-9 available online at http://www.idealibrary.com on IDEAL® J. Mol. Biol. (2002) 324, 331–347

JMB

Differential Salt-induced Stabilization of Structure in the Initial Folding Intermediate Ensemble of Barstar

Lovy Pradeep and Jayant B. Udgaonkar*

National Centre for Biological Sciences, Tata Institute of Fundamental Research, GKVK Campus, Bangalore 560 065 India

The effects of two salts, KCl and $MgCl_2$, on the stability and folding kinetics of barstar have been studied at pH 8. Equilibrium urea unfolding curves were used to show that the free energy of unfolding, ΔG_{UN}, of barstar increased from a value of 4.7 kcal mol^{-1} in the absence of salt to a value of 6.9 kcal mol^{-1} in the presence of 1 M KCl or 1 M $MgCl_2$. For both salts, ΔG_{UN} increases linearly with an increase in concentration of salt from 0 M to 1 M, suggesting that stabilization of the native state occurs primarily through a Hofmeister effect. Refolding kinetics were studied in detail in the presence of 1 M KCl as well as in the presence of 1 M $MgCl_2$, and it is shown that the basic folding mechanism is not altered upon addition of salt. The major effects on the refolding kinetics can be attributed to the stabilization of the initial burst phase ensemble, I_E, by salt. Stabilization of structure in I_E by KCl causes the fluorescence properties of I_E to change, so that there is an initial burst phase change in fluorescence at 320 nm, during refolding. The structure in I_E is stabilized by $MgCl_2$, but no burst phase change in fluorescence at 320 nm is observed during refolding. The fluorescence emission spectra of I_E show that when refolding is initiated in 1 M KCl, the three tryptophan residues in I_E are less solvent exposed than when folding is initiated in 1 M $MgCl_2$. Stabilization of I_E leads to an acceleration in the rate of the fast observable phase of folding by both salts, suggesting that structure of the transition state resembles that of I_E. The stabilization of I_E by salts can be accounted for largely by the same mechanism that accounts for the stabilization of the native state of the protein, namely through the Hofmeister effect. The salts do not affect the rates of the slower phases of folding, indicating that the late intermediate ensemble, I_L, is not stabilized by salts. Stabilization of the native state results in deceleration of the fast unfolding rate, which has virtually no dependence on the concentration of KCl or $MgCl_2$ at high concentrations. The observation that the salt-induced stabilization of structure in I_E is accompanied by an acceleration in the fast folding rate, suggests that I_E is likely to be a productive on-pathway intermediate.

Keywords: salt-induced protein stabilization; Hofmeister effect; burst phase intermediate; protein folding; protein electrostatics

*Corresponding author

Introduction

An important and currently contentious issue in protein folding concerns the following question: do the changes in protein conformation that occur immediately upon transferring a polypeptide chain from a high concentration of denaturant (unfolding conditions) to a low concentration (refolding conditions) signify the formation of an intermediate with at least some specific structure or do they merely represent a non-specific collapse of the chain consequent to change from good to bad solvent? For ribonuclease A[1] as well as cytochrome *c*,[2,3] it has been observed that the fractional change in optical signals that occurs upon denaturant dilution for the unfolded protein is the same as what occurs upon denaturant dilution during a folding reaction. This suggests that the collapse processes that occur during the folding of these proteins are identical with those seen during denaturant dilution of unfolded protein. Nevertheless, it has not been shown explicitly that

Abbreviations used: ANS, 8-anilino-1-naphthalene-sulphonic acid.

E-mail address of the corresponding author: jayant@ncbs.res.in

the two collapse processes are identical either in their kinetics or in the products they lead to. On the other hand, kinetic studies of the refolding of cytochrome *c* consequent to denaturant dilution suggest that the initial product is a productive folding intermediate and does not represent the unfolded state in refolding conditions.[4,5] The issue is further complicated because, for several proteins, the initial product of folding consequent to denaturant dilution is structurally heterogeneous,[4,6–11] presumably because of the existence of multiple folding pathways.[12]

One way to address the relevance of the initial product of folding upon denaturant dilution is to investigate how its structure changes upon a change in folding conditions that changes its stability. Intermediates on the folding and unfolding routes very often become discernible when environmental conditions such as solvent composition, pH, ionic strength and temperature are altered.[13–20] The ability of inorganic salts to stabilize the native states of protein is well known.[21] Salts are useful for characterizing partially structured intermediate states that populate refolding pathways, which can be induced to accumulate transiently at sufficiently high concentrations of salt.[22,23] Intermediates have been detected on folding pathways by the appearance of additional kinetic phases when folding is carried out in the presence of salts. For example, when hen egg-white lysozyme is refolded in the presence of ≥ 0.1 M NaCl, an additional kinetic phase is observed because a kinetic intermediate is stabilized at higher concentrations of salt.[24] A salt-induced collapsed state, which is populated during the refolding of the ribosomal protein S6 from *Thermus thermophilus* in the presence of Na_2SO_4, has been suggested to be a prematurely collapsed form that is off-pathway because it slows folding by several orders of magnitude.[25] The use of high concentrations of KCl contributed to the detection of multiple kinetic intermediates on the unfolding routes of barstar.[26]

The 89 amino acid residues, single-domain protein, barstar, is the intracellular inhibitor of the extracellular RNase, barnase, in the bacterium *Bacillus amyloliquefaciens*. Barstar has two proline residues at positions 27 and 48. In the N state, the N-aminoacyl bond of Pro27 is in the *trans* conformation whereas Pro48 is in the *cis* conformation. Unfolded barstar has U_F and U_S in equilibrium in a 30:70 ratio, where U_F is the fast folding unfolded form that has the Tyr47-Pro48 bond in the native-like *cis* conformation and U_S is the slow folding unfolded form with the Tyr47-Pro48 bond in the non-native *trans* conformation.[27,28] The folding mechanism of barstar has been characterized in detail[6,27–31] and three refolding routes are available at very low concentrations of denaturant:[6]

$$U_S \underset{fast}{\overset{very}{\rightleftharpoons}} I_{M1} \overset{fast}{\rightarrow} I_N \overset{slow}{\rightarrow} N$$
$$U_S \underset{fast}{\overset{very}{\rightleftharpoons}} I_{M2} \overset{fast}{\rightarrow} I_{S2} \overset{slow}{\rightarrow} N \qquad \text{Mechanism 1}$$
$$U_F \underset{fast}{\overset{very}{\rightleftharpoons}} I_{F1} \overset{fast}{\rightarrow} N$$

where I_{F1}, I_{M1} and I_{M2} are intermediates that form within the first few milliseconds after initiation of refolding. While these intermediates resemble the U form in lacking any secondary or tertiary structure as measured by circular dichroism (CD) or intrinsic tryptophan fluorescence, they also appear to be collapsed structures, as measured by fluorescence energy transfer or by 8-anilino-1-naphthalene-sulphonic acid (ANS) binding. The late, structured intermediates I_N and I_{S2} differ from the early intermediates in their fluorescence and CD properties. The major structural transitions are the fast steps in mechanism 1, and appear to occur with identical rate constants. Thus, the folding of barstar in strongly stabilizing conditions can be represented as:

$$U \overset{K_{UI}}{\rightleftharpoons} I_E \overset{k}{\rightarrow} I_L \overset{slow}{\rightarrow} N \qquad \text{Mechanism 2}$$

I_E represents an ensemble of early intermediates that equilibrate with U prior to the major structural transition to I_L, which represents an ensemble of late structured intermediates. I_E includes I_{M1}, I_{M2} and I_{F1}, while I_L includes I_N and I_{S2}, and it is likely that both ensembles consist of many more intermediates.[12]

Previous studies had indicated that barstar is stabilized considerably upon addition of 0.8 M KCl.[26] The mode of action of the salt was, however, not determined. Progressive addition of salt to the pH 12-unfolded D form of barstar, which has been shown to be as unfolded as the urea-unfolded U form,[32] leads first to a collapsed structureless, premolten globule form, which transforms into a more structured molten globule form at high concentrations of salt. The structured molten globule has been shown to be on the direct pathway of folding from the D form to the N state.[33] This study indicated that high concentrations of salt, acting through a Hofmeister effect,[34] play an important role in determining the structures of the early intermediates that separate the unfolded and molten globule forms. It is therefore important to determine whether high concentrations of salt play a similar role in determining the structure and stability of the very early intermediate ensemble I_E, which accumulates initially during the refolding of the urea-unfolded U form. It was of particular interest to determine whether different salts would differentially affect the structures present in I_E.

Here, it is first shown that the free energy of unfolding of the N state of barstar to the U form has a linear dependence on the concentration of KCl as well as of $MgCl_2$, suggesting that the mechanism of stabilization by both salts involves primarily the Hofmeister effect. Next, it is shown that the structure of the initial intermediate ensemble, I_E, is altered significantly in the presence of 1 M KCl. The alteration in structure results in the fluorescence properties of I_E in the presence of 1 M KCl being different from those of U; consequently, a burst phase change in fluorescence is

observed in the presence of 1 M KCl but not in its absence. Stabilization of I_E by the addition of KCl leads to acceleration of the major, fast folding reaction, the $I_E \rightarrow I_L$ reaction. Secondly, it is shown that $MgCl_2$ stabilizes I_E and, like KCl, causes an acceleration of the observable folding rate. From the fluorescence spectra of I_E determined when refolding is initiated in the presence of 1 M KCl, in the presence of 1 M $MgCl_2$ or in the absence of added salt, it appears that the structure stabilized by $MgCl_2$ in the burst phase ensemble is different from that stabilized by KCl, and from that seen in the absence of any salt. Finally, although both salts stabilize the N state strongly, unfolding rates are decreased to only a very small extent. The effect of either salt on the folding kinetics is on the steps involving formation of I_E and I_L and the rates of the kinetic phase corresponding to the $I_L \rightarrow N$ reaction are not affected by the presence of salt.

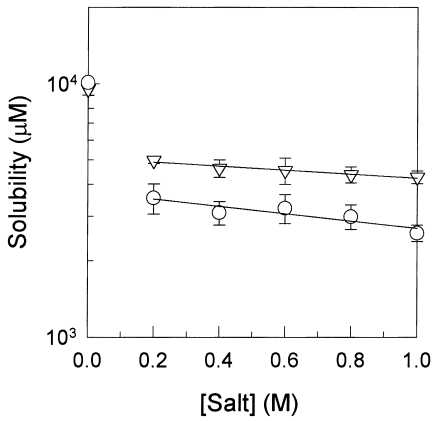

Figure 1. Dependence of solubility of barstar on salt concentration at 25 °C. Solubility measurements were made in varying concentrations of KCl (▽) and $MgCl_2$ (○). The continuous line through the data is drawn by inspection only.

Results

Optical spectroscopic properties of barstar are not affected in the presence of salt (KCl or $MgCl_2$)

Fluorescence and CD spectra in the absence and in the presence of KCl or $MgCl_2$ show that there is no shift in the emission maximum (λ_{max}) or mean residue ellipticity at 222 nm, respectively, for both the N and U forms (data not shown). The N state shows the same intrinsic fluorescence intensity in the absence and in the presence of 1 M KCl or 1 M $MgCl_2$, while the U form shows a 4% greater fluorescence intensity in the presence of 1 M KCl and an 8% greater fluorescence intensity in the presence of 1 M $MgCl_2$.

Dependence of solubility on salt concentration

Figure 1 shows that the solubility of barstar decreases with an increase in KCl or $MgCl_2$ concentration, marginally more so for the latter than for the former. A large decrease in solubility is seen between 0 M and 0.2 M salt, and above 0.2 M salt, the solubility decreases marginally with salt concentration. All experiments on the dependence of stability and refolding kinetics on the concentration of salt were done using protein concentrations at least tenfold lower than the solubility limit of the protein in 1 M KCl and 1 M $MgCl_2$.

Equilibrium urea-induced unfolding transitions in the absence and in the presence of KCl

Figure 2(a) compares urea-induced equilibrium unfolding transitions of barstar in the absence and in the presence of KCl, using tryptophan emission at 320 nm as a global probe. It is seen that C_m increases with KCl concentration. The data were fit to equation (5). The values of ΔG_{UN} and m_{UN} obtained in the absence of any KCl are similar to values reported earlier.[27] Similar results were obtained with far-UV CD at 222 nm (Figure 2(b)). Figure 2(c) shows plots of fraction unfolded, f_U, (equation (6)) with concentration of urea. At any concentration of salt, both probes yielded overlapping f_U plots, indicating simultaneous loss of secondary and tertiary structure, and supporting the assumption made in equations (5) and (7), that the U ⇌ N transition is two-state.

Dependence of the thermodynamics of urea-induced unfolding on the concentration of salt

Fluorescence-monitored urea-induced unfolding transitions, such as those shown in Figure 2(a), were determined at different concentrations of KCl and $MgCl_2$ in the range 0–1 M. Figure 3 shows the dependence of $\Delta G^{//}_{UN}$, m_{UN} and C_m on the concentration of KCl and $MgCl_2$. At any one concentration of salt, the value of any of these thermodynamic parameters is the same for both salts. The free energy of unfolding is seen to increase linearly from a value of 4.7(±0.1) kcal mol^{-1} (1 cal = 4.184 J) in the absence of salt to a value of 6.9(±0.1) kcal mol^{-1} in 1 M KCl or 1 M $MgCl_2$. The value of m_{UN} is −1.17(±0.02) kcal mol^{-1} M^{-1} in the absence of salt and remains unchanged with the increase in the concentration of KCl or $MgCl_2$ up to 1 M: the values at all concentrations of KCl and $MgCl_2$ are within three standard deviations of the value obtained in the absence of any salt, in support of the assumptions made in equation (4). The linear dependence of the free energy of unfolding on the concentration of KCl or $MgCl_2$ was fit to equation (3), which yielded a value of 2.2 kcal mol^{-1} M^{-1} for m_S^N.

Kinetics of refolding in the absence and in the presence of salt

Figure 4 shows the kinetic traces of refolding of barstar in 0.92 M urea in the absence of added

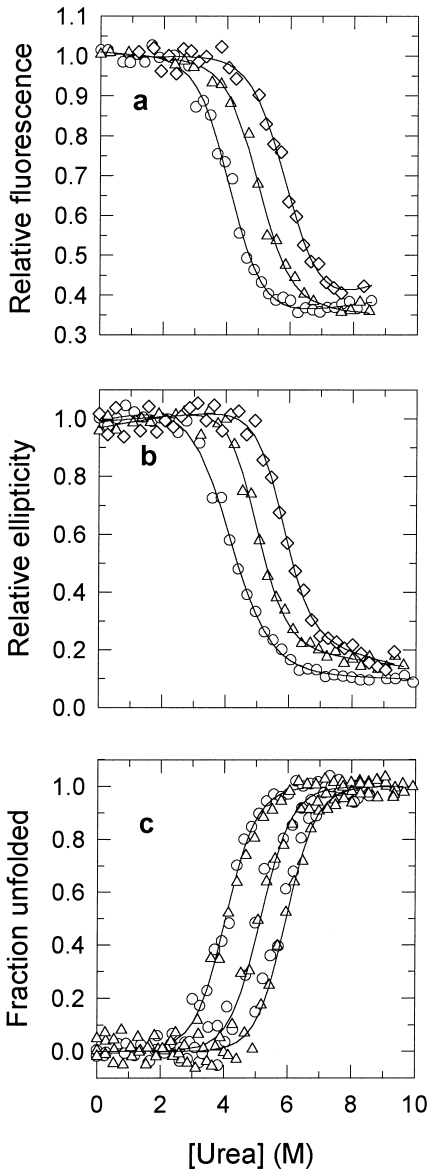

Figure 2. Stabilization of wild-type barstar by KCl at pH 8, 25 °C. (a) Equilibrium urea-induced unfolding transitions were determined using fluorescence at 320 nm to monitor unfolding in 0 M (○), 0.5 M (△) and 1 M KCl (◇). The unfolding transitions were fit to equation (5), and the fits, represented by the continuous lines, yielded values for $\Delta G''_{UN}$ and m_{UN} of 4.7 kcal mol^{-1} and −1.15 kcal mol^{-1} M^{-1} in 0 M KCl, 5.9 kcal mol^{-1} and −1.15 kcal mol^{-1} M^{-1} in 0.5 M KCl, and 6.9 kcal mol^{-1} and −1.2 kcal mol^{-1} M^{-1} in 1 M KCl, respectively. (b) Equilibrium urea-induced unfolding transitions were determined using mean residue ellipticity at 222 nm to monitor unfolding in 0 M (○), 0.5 M (△) and 1 M KCl (◇). The unfolding transitions were fit to equation (5), and the fits, represented by the continuous lines, yielded values for $\Delta G''_{UN}$ and m_{UN} of 4.9 kcal mol^{-1} and −1.17 kcal mol^{-1} M^{-1} in 0 M KCl, 5.5 kcal mol^{-1} and −1.12 kcal mol^{-1} M^{-1} in 0.5 M KCl, and 6.9 kcal mol^{-1} and −1.19 kcal mol^{-1} M^{-1} in 1 M KCl, respectively. (c) The raw data in (a) and (b) were converted to plots of f_U *versus* urea concentration using equation (6) and the data fit to equation (7). The fits are represented by the continuous lines through the data: (○) fluorescence and (△) MRE at 222 nm.

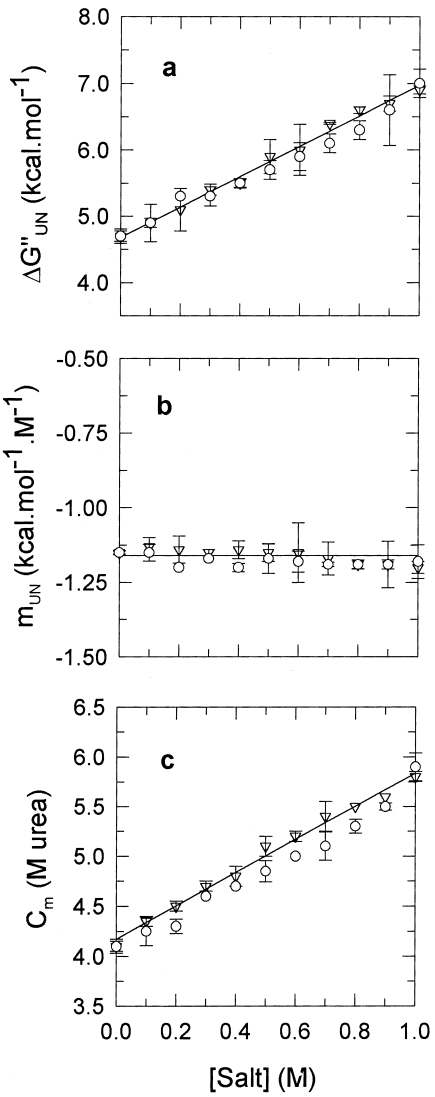

Figure 3. Effect of KCl and $MgCl_2$ on the thermodynamics of unfolding. (a) $\Delta G''_{UN}$, (b) m_{UN} and (c) C_m were determined from urea-induced unfolding transitions of barstar in KCl (▽) and $MgCl_2$ (○) at pH 8, 25 °C, monitored by fluorescence at 320 nm upon excitation at 280 nm. Error bars on the data points represent the spreads from two separate determinations. The continuous line through the data in (a) is a fit of the data to equation (3) and yields values for $\Delta G''_{UN}$ and m_S^N of 4.7 kcal mol^{-1} and 2.21 kcal mol^{-1}M^{-1}, the continuous line through the data in (b) represents the mean value of m_{UN}, (−1.17 kcal mol^{-1} M^{-1}), averaged over all salt concentrations and for both salts, and the continuous line through the data in (c) is described by, $C_{m\ (salt)} = 4.11 + 1.66$ [salt].

salt, in the presence of 1 M KCl and in the presence of 1 M $MgCl_2$. In previous studies of refolding in the absence of added salt, the refolding of urea-unfolded[27] as well as of GdnHCl-unfolded barstar[28] have been described as two-exponential processes. In Figure 4(a), it is seen, however, that the use of a three-exponential equation, with the inclusion of an additional kinetic phase, intermediate in rate between the fast and slow phases, significantly

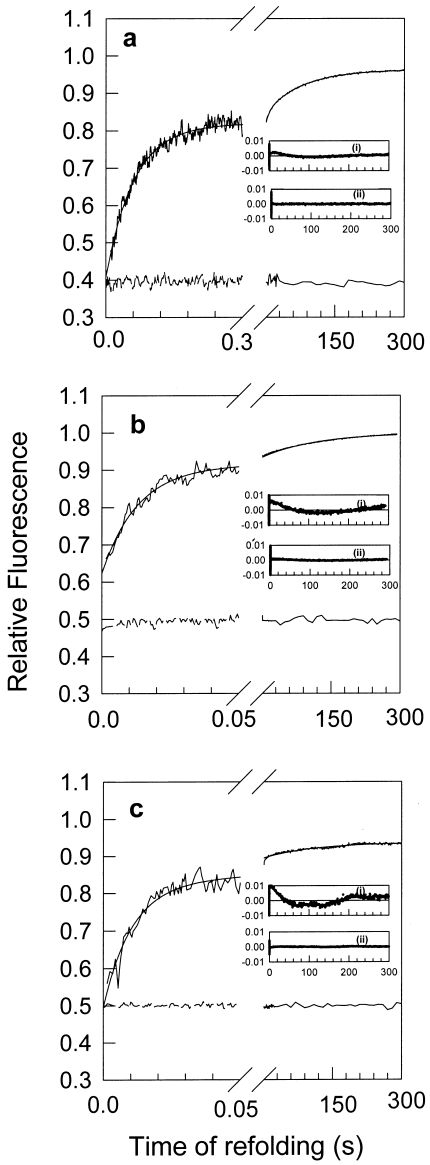

Figure 4. Kinetics of folding in 0.92 M urea (a) in the absence of salt, (b) in the presence of 1 M KCl, and (c) in the presence of 1 M $MgCl_2$. In each panel, the continuous line through the data is a least-squares fit of the data to equation (8). In each panel, inset (i) shows the residuals of a two-exponential fit to the data, and inset (ii) shows the residuals of a three-exponential fit to the data. The broken line indicates the signal of the unfolded protein at the same protein concentration.

improves the quality of the fit (Figure 4(a), insets). The relative amplitude of the intermediate phase is less than 5% of the total refolding amplitude at all concentrations of urea, which is probably why it was missed in the earlier studies. For describing refolding in the presence of 1 M KCl, the necessity for including the additional intermediate phase is more obvious (Figure 4(b), insets). Figure 4(b) shows that in the presence of 1 M KCl, there is an additional, unobservable burst phase change in fluorescence, which is complete in the first 1.4 ms (dead-time of mixing): the observable kinetic phases of refolding do not extrapolate to the signal corresponding to U at $t = 0$. In the presence of 1 M $MgCl_2$, the three observable kinetic phases account for the complete observed change in fluorescence (Figure 4(c)). In 0.92 M urea, the rates of the fast phase of refolding in 1 M KCl and 1 M $MgCl_2$, both $65(\pm 5)\ s^{-1}$, are considerably faster than the rate in the absence of salt, $17(\pm 3)\ s^{-1}$.

Figure 5(a)–(c) show that in the absence of salt, in the presence of 1 M KCl, and in the presence of 1 M $MgCl_2$, the fast rate of refolding increases with a decrease in concentration of urea. Figure 5(b) shows that the burst phase of fluorescence change increases in amplitude with a decrease in concentration of urea for folding in 1 M KCl. The observation that there is no burst phase change for folding in 1 M $MgCl_2$, even at the lowest concentration of urea studied, where the fast rate is comparable in magnitude to the fast rate observed in 1 M KCl, indicates that the burst phase seen in KCl is indeed real, and not an artifact of an incorrectly measured dead-time of mixing. Figure 5(d)–(f) indicate that unfolding rates increase with increasing concentration of urea, and that the observable kinetic phases account for the complete observed change in fluorescence during unfolding. It is seen that unfolding rates become only marginally slower in the presence of 1 M KCl or 1 M $MgCl_2$.

Burst phase changes in fluorescence during folding

The occurrence of a burst change in fluorescence at 320 nm, for folding in 1 M KCl but not in 1 M $MgCl_2$ or in the absence of any salt, as well as the absence of a burst phase change in fluorescence for unfolding in the absence or presence of salt, is best illustrated in Figure 6(a)–(c), where the kinetic amplitudes of folding and unfolding are compared with the equilibrium amplitudes over a wide range of concentrations of urea. In all cases, the end points ($t = \infty$) of the kinetic curves, whether folding or unfolding, fall on the equilibrium unfolding curves, indicating that each folding or unfolding reaction has been monitored to completion. The start points ($t = 0$) of the kinetic curves for refolding, obtained by extrapolation of the fits to the observed kinetic curves, both in the absence of salt and in the presence of 1 M $MgCl_2$, fall on the relevant linearly extrapolated unfolded protein baselines. The $t = 0$ points of the kinetic curves for unfolding in the absence as well as in the presence of either salt, fall on the respective linearly extrapolated native protein baselines. Only for refolding in 1 M KCl, do the $t = 0$ points of the kinetic refolding curves, not fall on the linearly extrapolated unfolded protein baseline: the sigmoidal dependence on the concentration of urea of the $t = 0$ points fit very well to equation (10). The values for ΔG_{UI}, m_{UI} and m_S^I (KCl), obtained from the fit, are given in the legend to Figure 6.

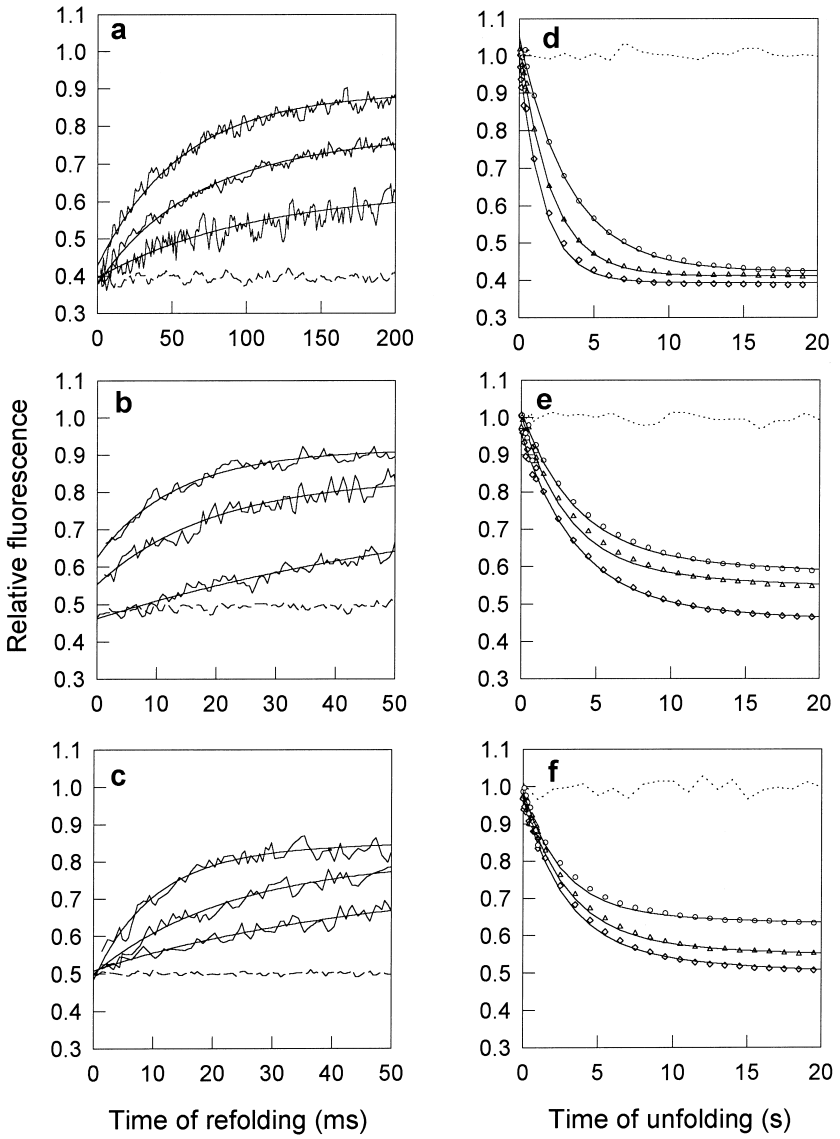

Figure 5. Kinetics of refolding and unfolding in 0 M, 1 M KCl and 1 M $MgCl_2$. (a) Kinetic traces of refolding in 0 M KCl. From top to bottom: representative normalized traces of refolding in three different concentrations of urea, 0.98 M, 1.63 M and 2.28 M, for the first 200 ms. (b) Kinetic traces of refolding in 1 M KCl. From top to bottom: representative normalized traces of refolding in three different concentrations of urea, 0.91 M, 2.1 M and 3.54 M, for the first 50 ms. (c) Kinetic traces of refolding in 1 M $MgCl_2$. From top to bottom: representative normalized traces of refolding in three different concentrations of urea, 1.02 M, 2.04 M and 3.74 M, for the first 50 ms. (d) Unfolding in 0 M KCl: representative normalized traces of unfolding in three different concentrations of urea, 6.5 M (○), 8.13 M (△) and 8.76 M (◇), for the first 20 seconds. (e) Unfolding in 1 M KCl: representative normalized traces of unfolding in three different concentrations of urea, 7.5 M (○), 7.8 M (△) and 8.8 M (◇), for the first 20 seconds. (f) Unfolding in 1 M $MgCl_2$: representative normalized traces of unfolding in three different concentrations of urea, 7.25 M (○), 7.88 M (△) and 8.5 M (◇), for the first 20 seconds. In each panel, fluorescence values have been normalized to a value of 1 for fully folded protein, the broken line indicates the signal of unfolded protein at the same protein concentration, and the dotted line indicates the signal of fully folded protein at the same concentration. The continuous lines through the data in (a)–(c) are fits to equation (8), and the continuous lines through the data in (d)–(f) are fits to equation (9).

Figure 6(d)–(f) compare the spectra of the product(s) of the burst phase during refolding in 0.92 M urea to the spectrum of the native protein dissolved in 0.92 M urea, and to the spectrum of the unfolded protein in 9.2 M urea, from which refolding was commenced. In each case, the spectrum of the burst phase product(s) was determined by obtaining kinetic refolding curves at the wavelengths indicated, and fitting these curves to equation (8). The spectrum of the burst phase product(s) for refolding in the absence of added salt was constructed by using the fitted value at $t = 5$ ms (Figure 6(d)), while for refolding in the presence of 1 M salt, the fitted value at $t = 2$ ms was used (Figure 6(e) and (f)). These times were chosen so that in all cases only 10(±2)% of the fluorescence change has occurred; in other words, the folding reactions in the three different refolding conditions have all proceeded to about the same extent. In the absence of any salt, the spectrum of the burst phase product(s) at 5 ms (Figure 6(d)) shows a maximum at 355 nm. In the presence of 1 M KCl, the spectrum of the burst phase product(s) at 2 ms shows a maximum at 345 nm, and is different from the spectrum of N, which shows a maximum at 337 nm and from the spectrum of U, which shows a maximum at 355 nm (Figure 6(e)). In the presence of 1 M $MgCl_2$, the spectrum of the burst phase product at 2 ms is again different from those of U and N, with a maximum at 350 nm (Figure 6(f)).

Urea dependence of the observable kinetics in the absence and in the presence of 1 M salt

Figure 7(a)–(c) show the rates and relative amplitudes of the observable kinetic phases of folding and unfolding, in the absence of salt.

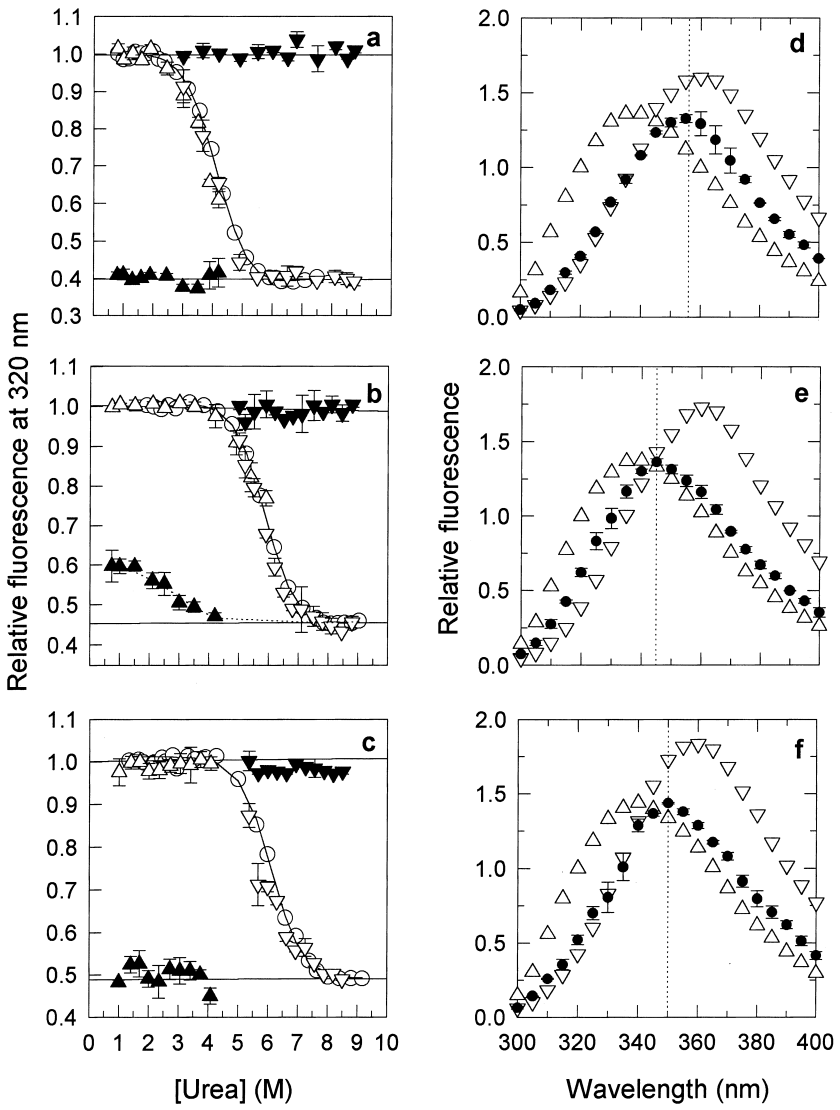

Figure 6. Burst phase changes in fluorescence during folding and unfolding at pH 8, 25 °C. Kinetic and equilibrium amplitudes of folding and unfolding are compared in (a) 0 M salt, (b) 1 M KCl and (c) 1 M $MgCl_2$. Urea-induced equilibrium unfolding curve (○); $t = 0$ points of kinetic folding traces (▲); $t = \infty$ points of kinetic folding traces (△); $t = 0$ points of kinetic unfolding traces (▼) and $t = \infty$ points of kinetic unfolding traces (▽). The continuous lines represent non-linear least-squares fits of the equilibrium unfolding data to equation (5). Error bars on the kinetic data points reflect the standard deviations determined from three repetitions of the experiment. (b) The $t = 0$ points of refolding in 1 M KCl are well accounted for by equation (10) (dotted line), and the fit yielded values for ΔG_{UI}, m_{UI} and m_S^I (KCl) of 0.5 kcal mol^{-1}, −0.95 kcal mol^{-1} M^{-1} and 2.9 kcal mol^{-1} M^{-1}, respectively. Fluorescence emission spectra upon excitation at 280 nm of the N state (△), the U form (▽), and the initial burst phase product at 5 ms of refolding in 0.92 M urea (●) in (d) 0 salt, at 2 ms of refolding in 0.92 M urea (●) in (e) 1 M KCl, and (f) 1 M $MgCl_2$. In each case, the N spectrum was determined under the same conditions as the spectrum of the burst phase product, while the U spectrum was determined in 9.2 M urea in the same conditions as the spectrum of the burst phase product. Error bars on the initial burst phase product (●) in (d)–(f) are standard deviations determined from three repetitions of the experiment.

Figure 7(d)–(f) do likewise for folding and unfolding in the presence of 1 M KCl, and Figure 7(g)–(i) do likewise for folding and unfolding in the presence of 1 M $MgCl_2$. The data obtained in the absence of salt are very similar to data reported earlier on the refolding of a mutant form of barstar,[27] except for the intermediate kinetic phase that is reported here.

A comparison of Figure 7(a), (d) and (g) indicates that upon addition of 1 M KCl or 1 M $MgCl_2$: (1) the fast rate constant for folding increases at all the concentrations of urea studied; (2) the curvature (roll-over) in the folding arm of the chevron is more pronounced; (3) the fast rate constants are well accounted for by equation (12) for refolding in urea concentrations below 3 M (up to 5 M in the presence of 1 M KCl and 1 M $MgCl_2$); (4) the fast rate constant for unfolding becomes only marginally slower at all concentrations of urea studied; (5) the chevron for the fast rate constant is shifted horizontally to the right to higher concentrations of urea, but not vertically; (6) the slope of the unfolding arm of the chevron is less and the unfolding rates have virtually no dependence on urea concentrations greater than 7 M; (7) the slow rate constant of folding and unfolding is not altered at any concentration of urea; and (8) the rate constant of the intermediate phase is no longer independent of the concentration of urea.

Comparisons of Figure 7(b) with (e) and (h), and 7(c) with (f) and (i), indicate that, upon addition of 1 M KCl or 1 M $MgCl_2$, (1) the relative amplitude of the fast phase and the slow phase shows a minimum (30%) and maximum (65–70%), respectively, at a higher concentration of urea (5.3 M in 1 M KCl; 5.4 M in 1 M $MgCl_2$) instead of at 3.5 M urea in the absence of salt; (2) the relative amplitudes of the fast as well as the slow phase are less at low concentrations of urea (only in 1 M KCl and not in 1 M $MgCl_2$) because of the presence of the burst

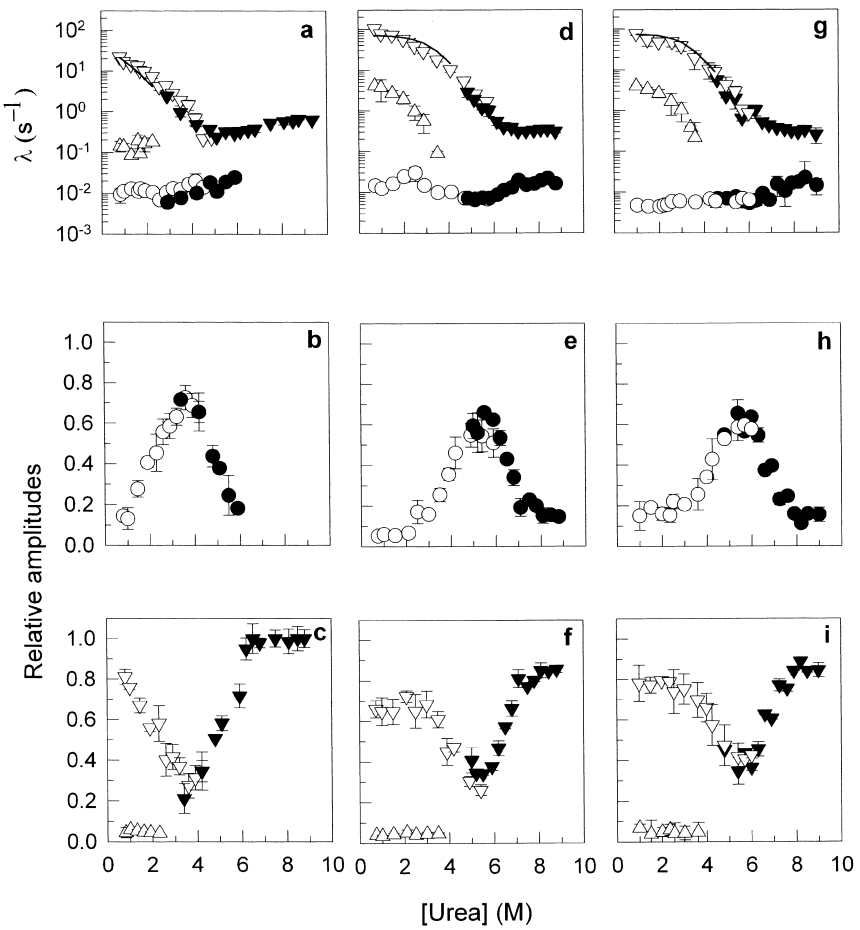

Figure 7. Urea dependence of the observable folding and unfolding kinetics at pH 8, 25 °C. The dependence of the logarithm of each of the folding and unfolding rates on the concentration of urea is shown (a) in the absence of any salt, (d) in the presence of 1 M KCl, and (g) in the presence of 1 M $MgCl_2$: fast refolding rate constant, λ_2 (▽), slow refolding rate constant, λ_1 (○) and intermediate refolding rate constant, λ_3 (△); fast unfolding rate constant, λ_2 (▼) and slow unfolding rate constant, λ_1 (●). Error bars on the points reflect the standard deviations from three repetitions of the experiment and, in most cases, the error bars are smaller than the symbols. The dependence on the concentration of urea of the relative amplitude (α_1) of the slow phase of refolding and unfolding is shown (b) in the absence of any salt, (e) in the presence of 1 M KCl, and (h) in the presence of 1 M $MgCl_2$: refolding, (○); unfolding (●). The dependence on the concentration of urea of the relative amplitudes of the fast (α_2) and intermediate phases (α_3) are shown for refolding and unfolding (c) in the absence of any salt, (f) in the presence of 1 M KCl, and (i) in the presence of 1 M $MgCl_2$: fast phase of refolding, (▽); fast phase of unfolding, (▼); intermediate phase of refolding, (△). The continuous lines through the data in (a), (d) and (g) are drawn according to equation (12) with values for k^0, m_k^D, m_k^S, ΔG_{UI}, m_{UI} and m_S^I of (a) 50 s^{-1}, 0 M^{-1}, 0 M^{-1}, 0.5 kcal mol^{-1}, −0.85 kcal mol^{-1} M^{-1} and 0 kcal mol^{-1} M^{-1}, respectively; (d) 50 s^{-1}, 0 M^{-1}, 0.35 M^{-1}, 0.5 kcal mol^{-1}, −1.0 kcal mol^{-1} M^{-1} and 2.8 kcal mol^{-1} M^{-1} respectively and (g) 50 s^{-1}, 0 M^{-1}, 0.43 M^{-1}, 0.5 kcal mol^{-1}, −1.0 kcal mol^{-1} M^{-1} and 2.8 kcal mol^{-1} M^{-1}, respectively. Error bars on the points are standard deviations determined from three repetitions of the experiment.

phase; (3) the relative amplitude of the fast phase of unfolding at the highest concentrations of urea is no longer 100% but is reduced to 85% because the slow phase is seen in the transition zone of unfolding and in the post-transition zone; and (4) the relative amplitude of the intermediate phase does not change and remains independent of the concentration of urea.

Salt-dependence of refolding and unfolding kinetics

Figure 8(a) shows the dependence of the observed rate constant of the fast phase of refolding in 0.92 M urea on the concentration of KCl, and Figure 8(b) does likewise for the dependence on the concentration of $MgCl_2$. In both cases, the dependence on salt concentration is well accounted for by equation (12), with values for ΔG_{UI}, m_{UI}, m_S^I (KCl) of 0.5 kcal mol^{-1}, −1.0 kcal $mol^{-1}M^{-1}$, 3.0 kcal $mol^{-1}M^{-1}$, and ΔG_{UI}, m_{UI}, m_S^I ($MgCl_2$) of 0.5 kcal mol^{-1}, −1.0 kcal $mol^{-1}M^{-1}$, 3.0 kcal mol^{-1}-M^{-1}, respectively (see the legend to Figure 8).

Figure 8(c) shows that the relative amplitude of the burst phase change in fluorescence, which occurs during refolding in 0.92 M urea, has a sigmoidal dependence on the concentration of KCl. This dependence is well described by equation

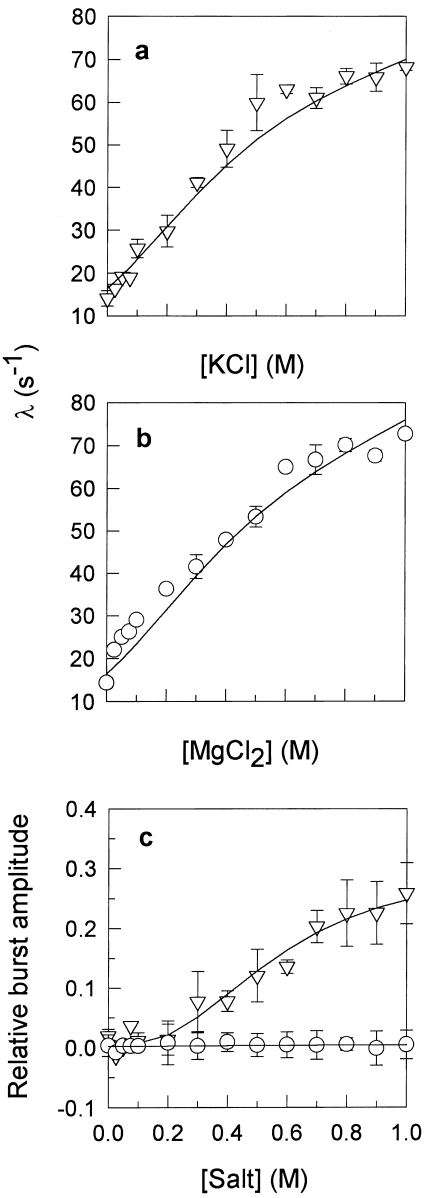

Figure 8. Salt concentration-dependence of fast refolding rates and burst phase amplitudes. The protein was refolded in 0.92 M urea at pH 8. (a) Dependence of fast refolding rate constant, λ_2, on KCl concentration. The continuous line through the data is drawn according to equation (12) with values for k^0, m_k^D, m_k^S, ΔG_{UI}, m_{UI} and m_S^I of 50 s^{-1}, 0 M^{-1}, 0.35 M^{-1}, 0.5 kcal mol^{-1}, −1.0 kcal mol^{-1} M^{-1} and 3.0 kcal mol^{-1} M^{-1}, respectively. (b) Dependence of fast refolding rate constant, λ_2, on $MgCl_2$ concentration. The continuous line through the data is drawn according to equation (12) with values for k^0, m_k^D, m_k^S, ΔG_{UI}, m_{UI} and m_S^I of 50 s^{-1}, 0 M^{-1}, 0.43 M^{-1}, 0.5 kcal mol^{-1}, −1.0 kcal mol^{-1} M^{-1} and 3.0 kcal mol^{-1} M^{-1}, respectively. (c) Dependence of relative amplitude of the burst phase, α_4, on the concentration of KCl (▽) and on the concentration of $MgCl_2$ (○) during refolding in 0.92 M urea. The continuous line through the dependence on the concentration of KCl is drawn according to equation (10), with values for ΔG_{UI}, m_{UI} and m_S^I (KCl) of 0.5 kcal mol^{-1}, −1.0 kcal $mol^{-1}M^{-1}$ and 2.8 kcal mol^{-1} M^{-1}, respectively. The continuous line through the $MgCl_2$ data is drawn by inspection only. Error bars on the data points are standard deviations determined from three separate determinations.

(10), with values of ΔG_{UI}, m_{UI}, and m_S^I (KCl) of 0.5 kcal mol^{-1}, −1.0 kcal $mol^{-1}M^{-1}$, 2.8 kcal mol^{-1}-M^{-1}, respectively (see the legend to Figure 8). These values are similar to those obtained from the dependence of the fast rate constant on the concentration of KCl in 0.92 M urea (Figure 8(a)) or from the dependence of the burst phase change in fluorescence on the concentration of urea, for refolding in 1 M KCl (Figure 6(b)).

The apparent rate constants of the intermediate and slow phases of refolding in 0.92 M urea are independent of the concentration of KCl or $MgCl_2$ (data not shown).The relative amplitude of the fast phase of refolding in 0.92 M urea is independent of the concentration of KCl, while the relative amplitudes of the slow and intermediate phases decrease at the expense of the increase in the burst phase amplitude. The relative amplitudes of the fast, intermediate and slow phases of refolding in 0.92 M urea are independent of the concentration of $MgCl_2$ (data not shown).

Discussion

Mechanism of salt-induced stabilization of barstar

Three mechanisms can be proposed for the observed salt-induced stabilization of barstar. The first mechanism invokes specific binding of cations to the native state of the protein. The importance of surface charges in determining protein stability is well known,[35–38] and the locations of charges on proteins appear to be optimized so that repulsive charge–charge interactions are avoided.[39] Salts are known to stabilize native proteins at low pH through specific anion binding.[40–43] Barstar has a charge of −6 at pH 8, and specific binding of K^+ or Mg^{2+} is expected to reduce the net negative charge on the protein. The binding surface of barstar, through which it interacts with barnase, has a cluster of four negatively charged residues, and replacement of any one of these with alanine results in an increase in stability.[44] Similarly, removal of unfavourable electrostatic interactions on the surface of the tenth fibronectin type III domain of human fibronectin by mutagenesis,[45] leads to protein stabilization.

Three observations argue against a specific cation binding effect being solely responsible for the observed stabilization: (1) specific ion-binding interactions usually occur at low concentrations of salts, usually below 0.2 M,[46,47] and for specific binding, ΔG_{UN} is expected to have a linear dependence on the logarithm of salt concentration.[48] Instead, the stabilization of barstar by KCl or $MgCl_2$ increases linearly with the concentration of salt over the entire range, 0–1 M. (2) At pH 9.8 where the protein has a charge of −10, the magnitude of the increase in free energy, $\Delta\Delta G_{UN}$, upon addition of 0.5 M KCl or 1 M KCl is the same (1 kcal mol^{-1} and 2.1 kcal mol^{-1}, respectively) as at pH 8, where

the charge on the protein is −6 (data not shown), and (3) $\Delta\Delta G_{UN}$, upon addition of 1 M Mg^{2+} is the same as upon addition of 1 M K^+.

The second mechanism invokes Debye screening. Mobile ions can screen repulsive electrostatic interactions in the folded state, thereby lowering the free energy of the folded state, or they may screen favourable electrostatic interactions in the unfolded state thereby raising the free energy of the unfolded state. Debye screening effects are non-specific, depending only on the ionic strength and not on the nature of the ions. At an ionic strength of 1 M, the Debye screening distance, over which electrostatic interactions are dampened out by mobile ions, is about 3 Å, and this distance is inversely proportional to the square root of the ionic strength. In a previous study on the effect of ionic strength, varied by addition of NaCl, on the stability of barstar,[44] increased stability in the presence of the salt was ascribed to Debye screening of unfavourable electrostatic interactions in the native state. Only one salt was, however, used in that study. Here, it is shown, by using two different salts, KCl and $MgCl_2$, that stabilization does not occur purely through a Debye screening mechanism. The ionic strength of a solution of $MgCl_2$ is three times that of an equimolar solution of KCl; nevertheless, equal concentrations of the two salts stabilize barstar to similar extents (Figure 3).

The third mechanism invokes the Hofmeister effect. At high concentrations, usually greater than 0.1 M, many salts are known to stabilize proteins as well as to decrease their solubility,[49–51] by increasing the strength of hydrophobic interactions. The observation that this effect is seen only at high concentrations of salts suggests that the interactions of salts with proteins are weak and non-specific.[52] According to the weak interaction model[53] for describing Hofmeister ion interactions with a protein, the salt acts as a chemical perturbant[54] and increases the chemical potential of the protein. The observation that ΔG_{UN} increases linearly with an increase in the concentration of salt (Figure 3), validates the use of the weak interaction model for describing the interaction of KCl or $MgCl_2$ with barstar.

The Hofmeister effect appears to originate in the ability of the salt to perturb the structure and hydrogen bonding properties of water.[51] The perturbation leads to an increase in surface tension, which in turn leads to preferential exclusion of the salt from the protein–water interface.[55] Such salts that interact unfavourably with the protein surface will tend to decrease solubility and unfolding so that the minimum surface is presented to the solvent. Since the unfolded form has a larger solvent-exposed surface than the native state, the degree of preferential exclusion is greater for the unfolded form than for the native state; hence, the increase in chemical potential of the unfolded form is more than it is for the folded state. The native state is therefore thermodynamically favoured over the unfolded form in the presence of salt, and the protein is stabilized.

The stabilization of barstar by KCl or $MgCl_2$ cannot be occurring only through a simple Hofmeister effect. If it did, then the degree of stabilization by 1 M concentrations of the two salts would not be the same, as is observed, but would be expected to be very different, because addition of 1 M $MgCl_2$ raises the surface tension of water 2.5 times more than does addition of 1 M KCl. Usually, a good correlation is seen between the experimentally measured negative preferential interaction of the co-solvent with the protein, and the positive surface tension increment,[56,57] but this is not always so.[55] For a divalent cation salt such as $MgCl_2$, the propensity of the salt to act as a salting-out or salting-in co-solvent, appears to be governed by a fine balance between preferential hydration due to the effect of the salt on the surface free energy of water, and the weak binding of the divalent cation to the protein.[57] At present, it is not possible to determine why the two salts at equal concentrations affect the stability to identical extents, or why the two salts decrease the solubility of barstar to almost similar extents (Figure 1), but it appears that specific weak binding of either cation may play a role. The stabilization of ribonuclease T_1 by salts has been attributed to the weak preferential binding of cations to the native state.[58]

The folding mechanism is not altered in the presence of salt

A comparison of the folding kinetics in the absence and in the presence of 1 M KCl or 1 M $MgCl_2$ (Figure 7) indicates that the folding mechanism of barstar is unaffected by the presence of salt. Most effects due to the presence of KCl can be accounted for either by the increase in stability of the native state upon addition of the salt (Figure 3), or by invoking an increase in the stability of folding intermediates known to exist on the folding pathway of barstar (mechanism 2). Thus, for example, the midpoint of the chevron for the fast phase is shifted from about 4.3 M urea in the absence of salt to about 6 M in 1 M KCl or 1 M $MgCl_2$, and the relative amplitude of the slow phase is shifted from being centred at about 3.5 M urea in the absence of salt to being centred at about 5.3 M in 1 M KCl and 5.4 M in 1 M $MgCl_2$. These shifts are equal to the shift seen in the value of C_m, the midpoint of equilibrium unfolding curves of the fully folded protein, which shifts from 4.1 M urea in the absence of salt to 5.8 M in 1 M KCl and 5.9 M in 1 M $MgCl_2$. The observation that fast unfolding rates are slower and the fast folding rates are faster in 1 M KCl or 1 M $MgCl_2$, than in the absence of added salt can be attributed to the observed increase in the stability of N.

The major difference in the observed kinetics is the presence of a sub-millisecond burst phase change in fluorescence for folding in the presence of 1 M KCl, which is not seen for folding in the

absence of added salt or for folding in the presence of 1 M $MgCl_2$. The burst phase change in fluorescence for folding in 1 M KCl must signify the formation of the burst phase folding intermediate ensemble (I_E) within the first 1.4 ms of folding. While it might appear that the absence of a burst phase change in fluorescence indicates that such a burst phase folding ensemble does not form in the absence of added salt or in the presence of 1 M $MgCl_2$, there is, in fact, strong evidence from previous studies for the formation of a burst phase intermediate ensemble, I_E, even in the absence of added salt.

Properties of the intermediate I_E in the absence of salt

In earlier experiments, in which the refolding of barstar was carried out in low concentrations of denaturant, the formation of I_E in an initial 5 ms burst phase had been indicated by several observations. (1) In fluorescence resonance energy transfer experiments, a major fraction of the final efficiency of energy of transfer of the folded state was recovered within the initial 5 ms of folding,[31] suggesting that the unfolded polypeptide chain collapses within 5 ms; (2) an increase in fluorescence of the hydrophobic dye ANS was seen to be complete within the initial 5 ms, suggesting that the collapsed form, I_E, has exposed hydrophobic patches capable of binding ANS;[6,31] and (3) kinetic studies could not predict the equilibrium free energy of unfolding, ΔG_{UN}.[6,27,28] The initial formation of I_E was, however, observed not to be accompanied by any change in fluorescence at 320 nm,[27,28] suggesting that the tryptophan residues in I_E are as hydrated as they are in U. In marginally stabilizing conditions (in the presence of 1 M GdnHCl), the initial intermediate ensemble I_E was found to be devoid of any helical secondary structure, and it was suggested that I_E is a compact but structureless globule.[31]

The observation of a burst phase change in fluorescence at 320 nm for folding in the presence of 1 M KCl, but not in the presence of 1 M $MgCl_2$ or in the absence of added salt, therefore suggests that the fluorescence properties of I_E are different in the absence of added salt, in the presence of 1 M KCl, and in the presence of 1 M $MgCl_2$. To confirm this, fluorescence spectra of the product(s) of the burst phase were collected (Figure 6). These confirm that I_E is structurally distinct in each of the three conditions chosen for the refolding studies.

Properties of I_E in the presence of 1 M salt

The spectra of the initial product(s) of folding in the absence of added salt, in the presence of 1 M KCl, and in the presence of 1 M $MgCl_2$, are compared to the spectra of N and U in Figure 6(d)–(f). In the absence of added salt, the wavelength of maximum emission, λ_{max}, of the burst phase product, I_E, is 355 nm, which is also the λ_{max} for U (356 nm). The maximum fluorescence intensity of I_E is, however, different from that of U. Moreover, the emission spectrum of I_E cannot be represented as a weighted sum of the emission spectra of N and U. In the presence of 1 M KCl, the λ_{max} of I_E is 345 nm, which is 11 nm blue-shifted from that of the U state and 8 nm red-shifted from that of the N state. In the presence of 1 M $MgCl_2$, the λ_{max} of I_E is 350 nm, which is 6 nm blue-shifted from that of the U state and 13 nm red-shifted from that of the N state. Clearly, in the presence of 1 M KCl or 1 M $MgCl_2$, the fluorescence spectrum of I_E cannot be represented as a weighted sum of the emission spectra of N and U, confirming that I_E is distinct from N and U. It appears from the λ_{max} values of I_E under different solvent conditions that the tryptophan residues are fully solvent exposed in the absence of salt, partially buried in the presence of 1 M $MgCl_2$, and even more buried (but not as buried as in N) in the presence of 1 M KCl. Thus, it appears that KCl as well as $MgCl_2$, each to a different extent, induce and stabilize additional structure in the I_E ensemble.

Stabilization of I_E in the presence of salt

In the absence of salt, I_E has been shown to be a molten globule-like intermediate in that it possesses hydrophobic patches to which ANS can bind.[6] The stabilization of acid-induced molten globule forms of proteins by specific anion binding is well known,[59–64] and the stabilities of the molten globule forms of cytochrome *c*[63] and apomyoglobin[64] at acidic pH are strongly dependent on the net charge on the protein.

Here, the stabilization of I_E, as of N (see above), is assumed to occur primarily through a Hofmeister effect, and ΔG_{UI} is assumed to have a linear dependence on salt concentration in the range 0–1 M. It is likely that the two salts (cations) bind to I_E also. In fact, an initial intermediate ensemble such as I_E is more likely than N to have repulsive charges in juxtaposition (see above), and specific binding of cations to I_E may play a relatively larger role in stabilizing I_E than does specific binding of cations to N. The observation that for either salt, m_S^I, is larger in value than m_S^N, strongly supports such an argument. Nevertheless, the assumption of a linear dependence of ΔG_{UI} on salt concentration appears to be broadly valid: equations (10) and (12) appear to describe satisfactorily the salt-dependence of folding kinetics at a fixed urea concentration, and the urea-dependence of folding kinetics at a fixed concentration of salt, and consistent values for ΔG_{UI}, m_{UI}, m_S^I, k^0, m_k^D, and m_k^S account for the data in Figures 6–8 (see Results and the Figure legends).

Like acid molten globule forms, the initial molten globule ensemble I_E is expected to be largely devoid of the specific side-chain interactions that characterize native forms of proteins. It is likely that the ensemble I_E consists of many different forms, some less structured and some more structured, and that in the absence of salt,

the less structured forms are thermodynamically favoured because of repulsion between negative charges. In the presence of salt, when hydrophobic interactions are strengthened by the Hofmeister effect, and when repulsion between negative charges are reduced by the presence of positive charges, either free or bound, it appears that more structured members of the I_E ensemble are thermodynamically favoured, and the degree of formation and stabilization of structure is dependent on the specific cation present. Multiple structurally distinct, collapsed states have been observed to accumulate initially during the folding of lysozyme.[7] Both collapsed and extended conformations appear to accumulate initially during the folding of ribonuclease A[8,9] as well as of cytochrome *c*,[4,10] indicating that structural heterogeneity might be a common feature of the initial intermediate ensembles that are the products of sub-millisecond folding events of many proteins.

The formation and stabilization of structure in I_E by the addition of KCl or $MgCl_2$ has important consequences on the observed folding kinetics. (1) An initial burst phase change in fluorescence is seen during folding in 1 M KCl because the I_E ensemble is sufficiently structured that its fluorescence at 320 nm differs from that of U (Figure 5(b)). (2) No initial burst phase change in fluorescence is seen during folding in 1 M $MgCl_2$ because I_E is not sufficiently structured in $MgCl_2$ for its fluorescence at 320 nm to differ from that of U (Figure 5(c)). (3) Since the degree of stabilization of I_E is dependent on the concentration of salt added (equation (3)), the magnitude of the burst phase change in fluorescence seen in the presence of KCl is dependent on the concentration of KCl (Figure 8(c)). (4) The observed rate of the fast phase of folding is increased in the presence of KCl (Figure 8(a)) and in the presence of $MgCl_2$ (Figure 8(b)), because the stabilization of I_E by the salt leads to greater accumulation of I_E, whose folding to I_L represents, to a large extent, the fast phase of folding. The increase in the fast rate is dependent on the concentration of KCl or $MgCl_2$ (Figure 8(a) and (b)) because the stabilization of I_E is dependent on the concentration of salt (equation (3)). (5) There is greater curvature (rollover) in the refolding arm of the chevron (Figure 7(a), (d) and (g)), where the folding rate in the presence of salt at any concentration of urea is given by equation (12), because the stabilization of I_E by salt has a larger effect on the folding rate at low concentrations of urea. Such rollovers in the refolding arms of chevrons have been seen for many proteins,[65–67] including barstar[27] at low concentrations of urea, where transient folding intermediates become sufficiently stable to populate to significant extents.

Validity of mechanism 2

It is observed that all kinetic data, including (1) the dependence on the concentration of urea of folding rates at 0 salt, 1 M KCl and 1 M $MgCl_2$ (Figure 7); (2) the dependence on the concentration of urea of the burst phase amplitude at 1 M KCl (Figure 6(b)); (3) the dependence on the concentration of KCl of the fast folding rate (Figure 8(a)); (4) the dependence on the concentration of KCl of the burst phase amplitude (Figure 8(c)); and (5) the dependence on the concentration of $MgCl_2$ of the fast folding rate (Figure 8(b)), can be described by equations (10)–(12), with consistent values for ΔG_{UI} and m_{UI}. This validates the use of mechanism 2, and equations (10)–(12), which follow from mechanism 2, to account for all the data, just as it also validates the use of the linear free energy model to account for the stabilization of the initial intermediate, I_E, by salt.

Relevance of I_E

Until now, the only evidence that I_E is structurally distinct from U had been that, I_E, unlike U, is capable of binding the hydrophobic dye ANS, attesting to its molten globule-like nature. An important question is whether the compaction of U to I_E merely reflects a non-specific collapse that accompanies a change from good (high concentration of denaturant) to bad (low concentration of denaturant) solvent, during folding. In other words, does I_E merely reflect U in low concentration of denaturant? A proper answer to this question will require determination of whether I_E contains any specific, native-like structure, or only non-native structure. In the case of cytochrome *c*, it has been suggested that a similar initially formed collapsed species is not really a productive intermediate as believed,[4,5] but is merely an unfolded form in refolding conditions.[2] However, very recent observations that not all folding cytochrome *c* molecules, but only a fraction of them, populate the collapsed species,[10,68] when it first forms and even at late times of folding, suggests that the collapsed species is indeed a productive intermediate separated from U by an energy barrier.[5] It remains to be seen for barstar whether I_E is populated completely at the time it is first formed, but it has been shown here that the structure of I_E, as measured by its fluorescence spectrum, is affected differently by the presence of different salts, which is a result more expected for a partially folded structure as found in a folding intermediate than for a completely unfolded form of a protein. Also importantly, I_E does indeed play the role of a productive intermediate: when it is stabilized by salt, folding rates are accelerated (Figures 5, 7 and 8), suggesting that its structure must resemble that of the transition state that follows it, because the latter must also be stabilized for the folding rate to increase.

Materials and Methods

Bacterial strain and plasmid, and protein purification

The *Escherichia coli* strain MM294 was used for protein expression. The expression plasmid for wt barstar was

pMT316 provided by R. W. Hartley. The method used to purify barstar has been described in detail.[69] Protein concentrations were calculated using an extinction coefficient of 23,000 M^{-1} cm^{-1}.[69] Mass spectroscopy using a Micromass Q-TOF Ultima instrument showed that the protein was pure with a mass of 10,342 Da, which indicated that the N-terminal methionine residue had remained uncleaved during synthesis.

Buffers and solutions

The native buffer used for all equilibrium and kinetic experiments was 30 mM Tris–HCl (pH 8) (ultrapure, 99.9% from GibcoBRL), 250 μM EDTA (disodium salt, dihydrate, 99 + % from SIGMA) and 250 μM DTT (ultrapure from GibcoBRL). Unfolding buffer was native buffer containing 9–10 M urea (ultrapure, 99.9% from USB). The concentrations of stock solutions of urea were determined by measuring the refractive index using an Abbe 3L refractometer from Milton Roy. For folding and unfolding studies in the presence of salt (KCl or $MgCl_2$), the salt was present in the refolding buffer as well as in the unfolding buffer. All buffers and solutions were filtered through 0.22 μm filters before use and were degassed prior to kinetic experiments.

Spectroscopic characterization

CD spectra were collected on a Jasco J720 spectropolarimeter, using a bandwidth of 1 nm, response time of one second, and a scan speed of 50 nm/minute. Each spectrum was an average of five scans monitored between 200 nm and 250 nm. The protein concentration used was 15 μM for the far-UV CD experiments, and the path-length of the cuvette was 0.1 cm. Fluorescence spectra were collected on a SPEX DM 3000 spectrofluorimeter. The protein was excited at 280 nm and the emission monitored between 300 nm and 400 nm with a bandwidth of 0.37 nm for excitation and 10 nm for emission. Each spectrum was an average of three scans. The protein concentration was typically 2–4 μM and the path-length of the cuvette used was 1 cm.

Equilibrium denaturation studies

Protein stability at equilibrium was determined by urea-induced denaturation studies using two probes. The CD at 222 nm and fluorescence at 320 nm were monitored as described above. Prior to the CD and fluorescence measurements, the samples were equilibrated for at least four hours. Identical results were obtained if the time of incubation was 24 hours.

Kinetic experiments

Kinetic experiments were performed on a Biologic SFM-4 stopped-flow mixing module. Folding and unfolding were monitored using intrinsic tryptophan fluorescence as the probe. The excitation wavelength was set at 280 nm, and emission was monitored at 320 nm using an Oriel bandpass filter with a bandwidth of 10 nm. The protein concentration during both refolding and unfolding was between 15 μM and 30 μM. In all experiments, an FC-08 cuvette with a path-length of 0.8 mm was used, the total flow-rate was 6.52 ml/second, and the dead-time of the instrument was 1.4 ms.

For refolding experiments, barstar was unfolded in 9–10 M urea (unfolding buffer) for at least four hours (the unfolding buffer contained KCl or $MgCl_2$ when refolding was studied in the presence of salt). In refolding experiments, the final concentration of urea was between 0.9 M and 3.8 M in the absence of salt, and between 0.9 M and 5.8 M in the presence of KCl or $MgCl_2$. For unfolding experiments, barstar was incubated in native buffer for at least four hours (the native buffer contained KCl or $MgCl_2$ when unfolding was studied in the presence of salt). In unfolding experiments, the final concentration of urea was between 3.0 M and 9.5 M in the absence of salt, and between 5.0 M and 9.5 M in the presence of KCl or $MgCl_2$.

Emission spectrum of the forms present at 2 ms and 5 ms of folding

A Biologic SFM-400 stopped-flow mixing module equipped with a monochromator (MOS-250) was used. The protein was excited at 280 nm. Fluorescence emission was monitored at wavelengths ranging from 300 nm to 400 nm for the refolding in 0.92 M urea of 25–30 μM barstar, in the presence of 1 M KCl or 1 M $MgCl_2$, or in the absence of added salt. An FC-08 cuvette was used, with typical flow-rates of 7.5 ml/second, and a dead-time of 1.2 ms. At each wavelength, the kinetic curve for folding was determined, fit to an exponential function, and the value of fluorescence at 2 ms (presence of salt) or 5 ms (absence of salt) was obtained. Emission spectra at 2 ms (presence of salt) or 5 ms (absence of salt) of refolding were constructed in this way. These were compared to the emission spectra of the native and the unfolded states obtained similarly in the absence of salt or in the presence of 1 M KCl or 1 M $MgCl_2$.

Solubility measurements

The solubility of the protein at different salt concentrations (both KCl and $MgCl_2$) was determined by measuring protein concentration using the Bradford colorimetric estimation method.

Data analysis

Solubility

The dependence of protein solubility (S) on the concentration of salt is described by the Setschenow equation,[70] when Hofmeister salt interactions with a protein can be described completely in terms of the weak interaction model:[49]

$$\log S = \log S(0) - K_S C_S \quad (1)$$

where $S(0)$ is the solubility of the protein in the absence of salt, C_S is the concentration of salt, and K_S is the salting-out coefficient.

Equilibrium and kinetic studies

According to the weak interaction (linear free energy) model for describing the interaction of urea (D) with a protein,[53,71] the change in free energy, $\Delta G'$, that occurs upon unfolding of any form of a protein, j, in the presence of D, is linearly dependent on denaturant concentration, [D]:

$$\Delta G'_{Uj} = \Delta G_{Uj} + m_{Uj}[D] \quad (2)$$

where m_{Uj} is the change in free energy associated with

the preferential interaction of the denaturant with the unfolded form, U, relative to the folded (partially or fully) form, j. When the form j is a partially folded intermediate I, $\Delta G_{UI}'$, represents the free energy of unfolding of I, and when j is the native state, N, $\Delta G_{UN}'$ represents the free energy of unfolding of N in the presence of denaturant. ΔG_{Uj} represents the free energy of unfolding of the folded (partially or fully) form j to U in the absence of any denaturant or added co-solute.

A Hofmeister salt, S, acting as a chemical perturbant, interacts with a protein according to the weak interaction model[48,49,72–74] and the free energy of unfolding of a folded form j to U, in the presence of S, is linearly dependent on salt concentration, [S]:

$$\Delta G''_{Uj} = \Delta G_{Uj} + m^{j}_{S}[S] \quad (3)$$

m_S^j is the change in free energy associated with the preferential interaction of the salt with the unfolded form, U, relative to the folded (partially or fully) form, j. According to equation (3), m_S^j has a positive value when the folded form is stabilized in the presence of salt. When the form j is a partially folded intermediate I, $\Delta G''_{UI}$ represents the free energy of stabilization of I, and when j is the native state, N, $\Delta G''_{UN}$ represents the free energy of stabilization of N, in the presence of salt.

Thus, in the presence of both denaturant and salt, the free energy of unfolding of a folded form, j to the unfolded form U, $\Delta G'''_{Uj}$ is given by:

$$\Delta G'''_{Uj} = \Delta G_{Uj} + m^{j}_{S}[S] + m_{Uj}[D] \quad (4)$$

Equation (4) assumes that m_{Uj} is independent of [S] and that m_S^j is independent of [D].

Equilibrium data for the unfolding of N as a function of [D], obtained in the presence of a fixed concentration of salt, were fit to a two-state U ⇌ N model according to the equation:

$$Y_0 = \frac{Y_N + m_N[D] + (Y_U + m_U[D])e^{\frac{-(\Delta G''_{UN} + m_{UN}[D])}{RT}}}{1 + e^{\frac{-(\Delta G''_{UN} + m_{UN}[D])}{RT}}} \quad (5)$$

where Y_0 is the value of the spectroscopic property being measured as a function of [D] at fixed [S], Y_N and Y_U represents the intercepts, and m_N and m_U the slopes, of the native protein and unfolded protein baselines, respectively. Thus, fits of denaturant-induced equilibrium unfolding data at different fixed values of [S] to equation (5), yield values for $\Delta G''_{UN}$ and m_{UN} at each fixed [S], and a subsequent fit of the salt-dependence of $\Delta G''_{UN}$ to equation (3) yields values for ΔG_{UN} and m_S^N.

Raw equilibrium unfolding data of N as a function of [D] were also analysed in an alternative way.[29] They were first converted to plots of fraction unfolded (f_U) *versus* [D], using equation (6) and the f_U values were then fit to equation (7):

$$f_U = \frac{Y_0 - (Y_N + m_N[D])}{(Y_U + m_U[D]) - (Y_N + m_N[D])} \quad (6)$$

$$f_U = \frac{e^{\frac{-(\Delta G''_{UN} + m_{UN}[D])}{RT}}}{1 + e^{\frac{-(\Delta G''_{UN} + m_{UN}[D])}{RT}}} \quad (7)$$

In equation (7), f_U is related to $\Delta G'''_{UN}$ by a transformation of the Gibbs–Helmholtz equation in which the equilibrium constant for unfolding in the transition zone, K'''_{UN}, is given by $K'''_{UN} = f_U/(1 - f_U)$, for a two-state transition.

The concentration of the denaturant at which the protein is half unfolded (when $\Delta G'_{Uj} = 0$), is given by C_m and from equation (2), $C_m = \Delta G_{Uj}/m_{Uj}$.

The observable kinetics of folding of barstar in the pre-transition zone are described by a three-exponential process:

$$A(t) = A(\infty) - A_1\, e^{-\lambda_1 t} - A_2\, e^{-\lambda_2 t} - A_3\, e^{-\lambda_3 t} \quad (8)$$

where $A(t)$ and $A(\infty)$ are the observed reduced amplitudes at time t and at infinity, λ_1, λ_2 and λ_3 are the apparent rate constants of the slow, fast and intermediate phases, and A_1, A_2 and A_3 are the respective amplitudes. The relative amplitude of each phase was determined by dividing the observed amplitude of that phase by the equilibrium amplitude of the reaction at that concentration of urea. In the transition zone, the folding process is two-exponential and is described by equation (8), with $A_3 = 0$.

The observable kinetics of unfolding in the transition zone and post-transition zone is described by a two-exponential process:

$$A(t) = A(\infty) + A_1\, e^{-\lambda_1 t} + A_2\, e^{-\lambda_2 t} \quad (9)$$

or by a single exponential process, by setting A_1 equal to zero in equation (9).

To analyse kinetic data according to Mechanism 2, it is assumed that the conformational transitions between U and I_E are rapid compared to the subsequent slow conversion of I_E to I_L and N, so that a transient pre-equilibrium, characterized by the equilibrium constant, K_{UI}, is established between U and I_E.

Thus, the pre-equilibrium data for the denaturant-induced unfolding of I_E, obtained from kinetic experiments in the presence of a fixed concentration of S, as well as the pre-equilibrium data for the salt-induced stabilization of I_E at a fixed concentration of denaturant, were fit to a two-state U ⇌ I_E model according to the equation:

$$Y_0 = \frac{Y_I + m_I[X] + (Y_U + m_U[X])e^{\frac{-(\Delta G_{UI} + m_{UI}[D] + m^{I}_{S}[S])}{RT}}}{1 + e^{\frac{-(\Delta G_{UI} + m_{UI}[D] + m^{I}_{S}[S])}{RT}}} \quad (10)$$

where [X] is the variable [D] for experiments in which refolding is carried out at a fixed value of [S], and [X] is the variable [S] for experiments in which refolding is carried out at a fixed [D]. Y_0 is the value of the spectroscopic property being measured as a function of the variable [X], Y_I and Y_U represent the intercepts, and m_I and m_U the slopes, of the I_E and U baselines, respectively.

The dependence of the rate constant, k, for the conversion of I_E to I_L or N (Mechanism 2) is expected to decrease exponentially with an increase in [D], because the free energy of activation is expected to increase linearly with an increase in [D]. Also, k is expected to increase exponentially with an increase in [S], because the free energy of activation is assumed to decrease linearly with an increase in [S]. This is given by the equation:

$$k = k^0\, e^{-m^{D}_{k}[D]}\, e^{m^{S}_{k}[S]} \quad (11)$$

where k° is the rate constant in the absence of denaturant and salt, RTm_k^D is the free energy associated with the preferential interaction of denaturant with the transition state relative to I_E, and RTm_k^S is the free energy associated with the preferential interaction of salt with the transition state relative to I_E.

Then, the observed rate of folding, λ''', in the presence of both urea at concentration [D] and salt at concentration [S], is given by:

$$\lambda''' = \frac{k}{1 + e^{\frac{-\Delta G'''_{UI}}{RT}}} = \frac{k^0 \, e^{-m_k^D[D]} \, e^{m_k^S[S]}}{1 + e^{\frac{-(\Delta G_{UI} + m_{UI}[D] + m_S^I[S])}{RT}}} \quad (12)$$

Acknowledgements

We thank members of our laboratory for discussion, and M. K. Mathew, B. R. Rami and R. Varadarajan for comments on the manuscript. J.B.U. is the recipient of the Swarnajayanti Fellowship from the Government of India. This work has been supported by the Tata Institute of Fundamental Research and the Department of Science and Technology, Government of India.

References

1. Qi, P. X., Sosnick, T. R. & Englander, S. W. (1998). The burst phase in ribonuclease A folding and solvent dependence of the unfolded state. *Nature Struct. Biol.* **5**, 882–884.
2. Sosnick, T. R., Shtilerman, M. D., Mayne, L. & Englander, S. W. (1997). Ultrafast signals in protein folding and the polypeptide contracted state. *Proc. Natl Acad. Sci. USA*, **94**, 8545–8550.
3. Bhuyan, A. K. & Udgaonkar, J. B. (1999). Relevance of burst phase changes in optical signals of polypeptides during protein folding. In *Perspectives in Structural Biology* (Vijayan, M., Yathindra, N. & Kolaskar, A. S., eds), pp. 293, Universities Press, Hyderabad.
4. Akiyama, S., Takahashi, S., Ishimori, K. & Morishima, I. (2000). Stepwise formation of alpha-helices during cytochrome *c* folding. *Nature Struct. Biol.* **7**, 514–520.
5. Shastry, M. C. R. & Roder, H. (1998). Evidence for barrier-limited protein folding kinetics on the microsecond time scale. *Nature Struct. Biol.* **5**, 385–392.
6. Shastry, M. C. R. & Udgaonkar, J. B. (1995). The folding mechanism of barstar: evidence for multiple pathways and multiple intermediates. *J. Mol. Biol.* **247**, 1013–1027.
7. Morgan, C. L., Miranker, A. & Dobson, C. M. (1998). Characterization of collapsed states in the early stages of the refolding of hen lysozyme. *Biochemistry*, **37**, 8473–8480.
8. Houry, W. A., Rothwarf, D. M. & Scheraga, H. A. (1996). Circular dichroism evidence for the presence of burst-phase intermediates on the conformational folding pathway of ribonuclease A. *Biochemistry*, **35**, 10125–10133.
9. Houry, W. A. & Scheraga, H. A. (1996). Structure of a hydrophobically collapsed intermediate on the conformational folding pathway of ribonuclease A probed by hydrogen–deuterium exchange. *Biochemistry*, **35**, 11734–11746.
10. Lyubovitsky, J. G., Gray, H. G. & Winkler, J. R. (2002). Mapping the cytochrome *c* folding landscape. *J. Am. Chem. Soc.* **124**, 5481–5485.
11. Nishimura, C., Jane Dyson, H. & Wright, P. (2002). The apomyoglobin folding pathway revisited: structural heterogeneity in the kinetic burst phase intermediate. *J. Mol. Biol.* **322**, 483–489.
12. Bhuyan, A. K. & Udgaonkar, J. B. (1999). Observation of multistate kinetics during the slow folding and unfolding of barstar. *Biochemistry*, **38**, 9158–9168.
13. Segawa, S. & Sugihara, M. (1984). Characterization of the transition state of lysozyme unfolding. I. Effect of protein–solvent interactions on the transition state. *Biopolymers*, **23**, 2473–2488.
14. Kuwajima, K., Mitani, M. & Sugai, S. (1989). Characterization of the critical state in protein folding. Effects of guanidine hydrochloride and specific Ca^{2+} binding on the folding kinetics of alpha-lactalbumin. *J. Mol. Biol.* **206**, 547–561.
15. Chen, B. L., Baase, W. A. & Schellman, J. A. (1989). Low-temperature unfolding of a mutant of phage T4 lysozyme. 2. Kinetic investigations. *Biochemistry*, **28**, 691–699.
16. Chen, B. L., Baase, W. A., Nicholson, H. & Schellman, J. A. (1992). Folding kinetics of T4 lysozyme and nine mutants at 12 °C. *Biochemistry*, **31**, 1464–1476.
17. Chen, X. & Matthews, C. R. (1994). Thermodynamic properties of the transition state for the rate-limiting step in the folding of the alpha subunit of tryptophan synthase. *Biochemistry*, **33**, 6356–6362.
18. Oliveberg, M., Tan, Y. J. & Fersht, A. R. (1995). Negative activation enthalpies in the kinetics of protein folding. *Proc. Natl Acad. Sci. USA*, **92**, 8926–8929.
19. Tan, Y. J., Oliveberg, M. & Fersht, A. R. (1996). Titration properties and thermodynamics of the transition state for folding: comparison of two-state and multi-state folding pathways. *J. Mol. Biol.* **264**, 377–389.
20. Agashe, V. R., Schmid, F. X. & Udgaonkar, J. B. (1997). Thermodynamics of the complex protein unfolding reaction of barstar. *Biochemistry*, **36**, 12288–12295.
21. von Hippel, P. H. & Schleich, T. (1969). The effects of neutral salts on the structure and conformational stability of macromolecules in solution. In *Structure and Stability of Biological Macromolecules* (Timasheff, S. N. & Fasman, G. D., eds), pp. 417, Marcel Dekker, New York.
22. Hamada, D., Hoshino, M., Kataoka, M., Fink, A. L. & Goto, Y. (1993). Intermediate conformational states of apocytochrome *c*. *Biochemistry*, **32**, 10351–10358.
23. Uversky, V. N., Karnoup, A. S., Segel, D. J., Seshadri, S., Doniach, S. & Fink, A. L. (1998). Anion-induced folding of Staphylococcal nuclease: characterization of multiple equilibrium partially folded intermediates. *J. Mol. Biol.* **278**, 879–894.
24. Bieri, O., Wildegger, G., Bachmann, A., Wagner, C. & Kiefhaber, T. (1999). A salt-induced kinetic intermediate is on a new parallel pathway of lysozyme folding. *Biochemistry*, **38**, 12460–12470.
25. Otzen, D. E. & Oliveberg, M. (1999). Salt-induced detour through compact regions of the protein folding landscape. *Proc. Natl Acad. Sci. USA*, **96**, 11746–11751.
26. Zaidi, F. N., Nath, U. & Udgaonkar, J. B. (1997). Multiple intermediates and transition states during protein unfolding. *Nature Struct. Biol.* **4**, 1016–1024.
27. Schreiber, G. & Fersht, A. R. (1993). The refolding of *cis*- and *trans*-peptidylprolyl isomers of barstar. *Biochemistry*, **32**, 11195–11203.

28. Shastry, M. C. R., Agashe, V. R. & Udgaonkar, J. B. (1994). Quantitative analysis of the kinetics of denaturation and renaturation of barstar in the folding transition zone. *Protein Sci.* **3**, 1409–1417.
29. Agashe, V. R. & Udgaonkar, J. B. (1995). Thermodynamics of denaturation of barstar: evidence for cold denaturation and evaluation of the interaction with guanidine hydrochloride. *Biochemistry*, **34**, 3286–3299.
30. Sridevi, K., Juneja, J., Bhuyan, A. K., Krishnamoorthy, G. & Udgaonkar, J. B. (2000). The slow folding reaction of barstar: the core tryptophan region attains tight packing before substantial secondary and tertiary structure formation and final compaction of the polypeptide chain. *J. Mol. Biol.* **302**, 479–495.
31. Agashe, V. R., Shastry, M. C. R. & Udgaonkar, J. B. (1995). Initial hydrophobic collapse in the folding of barstar. *Nature*, **377**, 754–757.
32. Rami, B. R. & Udgaonkar, J. B. (2001). pH-jump-induced folding and unfolding studies of barstar: evidence for multiple folding and unfolding pathways. *Biochemistry*, **40**, 15267–15279.
33. Rami, B. R. & Udgaonkar, J. B. (2002). Mechanism of formation of a productive molten globule form of barstar. *Biochemistry*, **41**, 1710–1716.
34. Hofmeister, F. (1888). Zur Lehre von der Wirkung der Salze. Zweite Mittheilung. *Arch. Expt. Pathol. Pharmakol.* **24**, 247–260.
35. Spector, S., Wang, M., Carp, S. A., Robblee, J., Hendsch, Z. S., Fairman, R. *et al.* (2000). Rational modification of protein stability by the mutation of charged surface residues. *Biochemistry*, **39**, 872–879.
36. Grimsley, G. R., Shaw, K. L., Fee, L. R., Alston, R. W., Huyghues-Despointes, B. M., Thurlkill, R. L. *et al.* (1999). Increasing protein stability by altering long-range coulombic interactions. *Protein Sci.* **8**, 1843–1849.
37. Perl, D., Mueller, U., Heinemann, U. & Schmid, F. X. (2000). Two exposed amino acid residues confer thermostability on a cold shock protein. *Nature Struct. Biol.* **7**, 380–383.
38. Loladze, V. V., Ibarra-Molero, B., Sanchez-Ruiz, J. M. & Makhatadze, G. I. (1999). Engineering a thermostable protein via optimization of charge–charge interactions on the protein surface. *Biochemistry*, **38**, 16419–16423.
39. Spassov, V. Z., Karshikoff, A. D. & Ladenstein, R. (1994). Optimization of the electrostatic interactions in proteins of different functional and folding type. *Protein Sci.* **3**, 1556–1569.
40. Makhatadze, G. I., Lopez, M. M., Richardson, J. M., III & Thomas, S. T. (1998). Anion binding to the ubiquitin molecule. *Protein Sci.* **7**, 689–697.
41. Uversky, V. N., Gillespie, J. R., Millett, I. S., Khodyakova, A. V., Vasiliev, A. M., Chernovskaya, T. V. *et al.* (1999). Natively unfolded human prothymosin alpha adopts partially folded collapsed conformation at acidic pH. *Biochemistry*, **38**, 15009–15016.
42. Bedell, J. L., McCrary, B. S., Edmondson, S. P. & Shriver, J. W. (2000). The acid-induced folded state of Sac7d is the native state. *Protein Sci.* **9**, 1878–1888.
43. Sakurai, K., Oobatake, M. & Goto, Y. (2001). Salt-dependent monomer–dimer equilibrium of bovine beta-lactoglobulin at pH 3. *Protein Sci.* **10**, 2325–2335.
44. Schreiber, G., Buckle, A. M. & Fersht, A. R. (1994). Stability and function: two constraints in the evolution of barstar and other proteins. *Structure*, **2**, 945–951.
45. Koide, A., Jordan, M. R., Horner, S. R., Batori, V. & Koide, S. (2001). Stabilization of a fibronectin type III domain by the removal of unfavourable electrostatic interactions on the protein surface. *Biochemistry*, **40**, 10326–10333.
46. Tanford, C. (1961). *Physical Chemistry of Macromolecules*, Wiley, New York pp. 346.
47. Jencks, W. P. (1987). Electrostatic interactions. In *Catalysis in Chemistry and Enzymology* (Jencks, W. P., ed.), pp. 351, Dover, New York.
48. Record, M. T., Jr, Zhang, W. & Anderson, C. F. (1998). Analysis of effects of salts and uncharged solutes on protein and nucleic acid equilibria and processes: a practical guide to recognizing and interpreting polyelectrolyte effects. Hofmeister effects, and osmotic effects of salts. *Advan. Protein Chem.* **51**, 281–353.
49. Baldwin, R. L. (1996). How Hofmeister ion interactions affect protein stability. *Biophys. J.* **71**, 2056–2063.
50. von Hippel, P. H. & Wong, K. Y. (1965). On the conformational stability of globular proteins. The effects of various electrolytes and nonelectrolytes on the thermal ribonuclease transition. *J. Biol. Chem.* **240**, 3909–3923.
51. Collins, K. D. & Washabaugh, M. W. (1985). The Hofmeister effect and the behaviour of water at interfaces. *Quart. Rev. Biophys.* **18**, 323–422.
52. Timasheff, S. N. (1993). The control of protein stability and association by weak interactions with water: how do solvents affect these processes? *Annu. Rev. Biophys. Biomol. Struct.* **22**, 67–97.
53. Schellman, J. A. (1990). A simple model for solvation in mixed solvents. Applications to the stabilization and destabilization of macromolecular structures. *Biophys. Chem.* **37**, 121–140.
54. Wyman, J. (1964). Linked functions and reciprocal effects in hemoglobin: a second look. *Advan. Protein Chem.* **19**, 223–286.
55. Kita, Y., Arakawa, T., Lin, T. Y. & Timasheff, S. N. (1994). ontribution of the surface free energy perturbation to protein–solvent interactions. *Biochemistry*, **33**, 15178–15189.
56. Arakawa, T. & Timasheff, S. N. (1982). Preferential interactions of proteins with salts in concentrated solutions. *Biochemistry*, **21**, 6545–6552.
57. Arakawa, T. & Timasheff, S. N. (1984). Mechanism of protein salting in and salting out by divalent cation salts: balance between hydration and salt binding. *Biochemistry*, **23**, 5912–5923.
58. Mayr, L. M. & Schmid, F. X. (1993). Stabilization of a protein by guanidinium chloride. *Biochemistry*, **32**, 7994–7998.
59. Goto, Y., Calciano, L. J. & Fink, A. L. (1990). Acid-induced folding of proteins. *Proc. Natl Acad. Sci. USA*, **87**, 573–577.
60. Hagihara, Y., Oobatake, M. & Goto, Y. (1994). Thermal unfolding of tetrameric melittin: comparison with the molten globule state of cytochrome *c*. *Protein Sci.* **3**, 1418–1429.
61. Goto, Y., Takahashi, N. & Fink, A. L. (1990). Mechanism of acid-induced folding of proteins. *Biochemistry*, **29**, 3480–3488.
62. Nishimura, C., Uversky, V. N. & Fink, A. L. (2001). Effect of salts on the stability and folding of staphylococcal nuclease. *Biochemistry*, **40**, 2113–2128.

63. Goto, Y. & Nishikori, S. (1991). Role of electrostatic repulsion in the acidic molten globule of cytochrome *c*. *J. Mol. Biol.* **222**, 679–686.
64. Kay, M. S. & Baldwin, R. L. (1998). Alternative models for describing the acid unfolding of the apomyoglobin folding intermediate. *Biochemistry*, **37**, 7859–7868.
65. Yamasaki, K., Ogasahara, K., Yutani, Y., Oobatake, M. & Kanaya, S. (1995). Folding pathway of *Escherichia coli* ribonuclease HI: a circular dichroism, fluorescence, and NMR study. *Biochemistry*, **34**, 16552–16561.
66. Raschke, T. M. & Marqusee, S. (1997). The kinetic folding intermediate of ribonuclease H resembles the acid molten globule and partially unfolded molecules detected under native conditions. *Nature Struct. Biol.* **4**, 298–304.
67. Parker, M. J. & Marqusee, S. (1999). The cooperativity of burst phase reactions explored. *J. Mol. Biol.* **293**, 1195–1210.
68. Akiyama, S., Takahashi, S., Kimura, T., Ishimori, K., Morishima, I., Nishikawa, Y. & Fujisawa, T. (2002). Conformational landscape of cytochrome *c* folding studied by microsecond-resolved small-angle X-ray scattering. *Proc. Natl Acad. Sci. USA*, **99**, 1329–1334.
69. Khurana, R. & Udgaonkar, J. B. (1994). Equilibrium unfolding studies of barstar: evidence for an alternative conformation which resembles a molten globule. *Biochemistry*, **33**, 106–115.
70. Setschenow, M. (1892). Action de l'acide carbonique sur les solutions dessels a acides forts. Etude absortiometrique. *Ann. Chim. Phys.* **25**, 226–270.
71. Schellman, J. A. (1987). The thermodynamic stability of proteins. *Annu. Rev. Biophys. Biophys. Chem.* **16**, 115–137.
72. Timasheff, S. N. (1998). Control of protein stability and reactions by weakly interacting cosolvents: the simplicity of the complicated. *Advan. Protein Chem.* **51**, 355–432.
73. Anderson, C. F. & Record, M. T., Jr (1993). Salt dependence of oligoion polyion binding—a thermodynamic description based on preferential interaction coefficients. *J. Phys. Chem.* **97**, 7116–7126.
74. Anderson, C. F. & Record, M. T., Jr (1995). Salt-nucleic acid interactions. *Annu. Rev. Phys. Chem.* **46**, 657–700.

Edited by C. R. Matthews

(Received 10 July 2002; received in revised form 23 September 2002; accepted 23 September 2002)